Development/Plasticity/Repair

BRI2 Inhibits Amyloid β-Peptide Precursor Protein Processing by Interfering with the Docking of Secretases to the Substrate

Shuji Matsuda,[1]* Luca Giliberto,[1]* Yukiko Matsuda,[1] Eileen M. McGowan,[2] and Luciano D'Adamio[1,3]

[1]Department of Microbiology and Immunology, Albert Einstein College of Medicine, Bronx, New York 10461, [2]Department of Neuroscience, Mayo Clinic College of Medicine, Jacksonville, Florida 32224, and [3]CEINGE Biotecnologie Avanzate, Dipartimento di Biochimica e Biotecnologie Mediche, Università di Napoli Federico II, 80145 Naples, Italy

Genetic alterations of amyloid β-peptide (Aβ) production caused by mutations in the Aβ precursor protein (*APP*) cause familial Alzheimer's disease (AD). Mutations in *BRI2*, a gene of undefined function, are linked to familial British and Danish dementias, which are pathologically and clinically similar to Alzheimer's disease. We report that BRI2 is a physiological suppressor of Aβ production. BRI2 restrict docking of γ-secretase to APP and access of α- and β-secretases to their cleavage APP sequences. Alterations of BRI2 by gene targeting or transgenic expression regulate Aβ levels and AD pathology in mouse models of AD. Competitive inhibition of APP processing by BRI2 may provide a new approach to AD therapy and prevention.

Key words: **amyloid-β; Alzheimer's disease; BRI2; familial dementia; synaptic plasticity; mice**

Introduction

Alzheimer's disease (AD), the most common cause of dementia in the world (Breteler et al., 1992), is characterized by cerebral atrophy, neurofibrillary tangles, and amyloid plaques in the hippocampus, entorhinal cortex, and other areas. Neurofibrillary tangles are intraneuronal helically wound filaments of hyperphosphorylated tau protein. Amyloid plaques are extracellular deposits of fibrillary amyloid β-peptide (Aβ), a peptide derived from processing of Aβ precursor protein (APP) (Selkoe and Podlisny, 2002; Selkoe and Kopan, 2003).

APP is a ubiquitous type I transmembrane protein that undergoes extensive proteolysis (Sisodia and St. George-Hyslop, 2002; Selkoe and Kopan, 2003). APP is first cleaved by β-secretase. Whereas the ectodomain [secreted APPβ (sAPPβ)] is released, the 99-aa-long C-terminal fragment (C99) remains membrane bound. C99 is cleaved by the γ-secretase. The γ-secretase consists of a multimolecular complex comprising Presenilins (PS1 and PS2), Nicastrin (NCT), PEN2, and APH1 (De Strooper, 2003). Two peptides are released. The amyloidogenic Aβ peptide, consisting of two major species of 40 and 42 aa (Aβ40 and Aβ42, respectively) and an intracellular product named APP intracellular domain that may regulate cell death (Passer et al., 2000), gene transcription (Cao and Südhof, 2001), and Ca^{2+} homeostasis (Leissring et al., 2002). Although Aβ40 represents the majority product, Aβ42 is the main Aβ species found in amyloid plaques because it is prone to oligomerization (Haass and Selkoe, 2007). In an alternative pathway, APP is cleaved by α-secretase within the Aβ sequence. Soluble APPα (sAPPα) and the membrane-bound C-terminal fragment of 83 aa (C83) are formed. Like C99, C83 is γ-secretase substrate.

After age, a positive family history of an AD-type dementia is the most important risk factor for AD, and 10–15% of all AD subjects have a family history consistent with an autosomal dominant trait. The latter cases are referred to as familial AD (FAD). Discovering that mutations in APP and in PS1/PS2 (Selkoe and Podlisny, 2002) cause FAD because they alter the rate of APP processing, genetically links APP processing to AD pathogenesis.

Given the physiopathological role of APP processing, we searched for regulators of APP cleavage and found that BRI2 binds APP and, if overexpressed in tumor cell lines, inhibits Aβ formation (Fotinopoulou et al., 2005; Matsuda et al., 2005). BRI2 is a type II membrane protein of 266 aa of unknown function that, remarkably, is mutated in autosomal dominant AD-like cerebral amyloidosis in familial British dementia (FBD) and familial Danish dementia (Vidal et al., 1999, 2000). BRI2 is cleaved at the C terminus (Kim et al., 1999; Choi et al., 2004). This cleavage generates a peptide of 23 aa plus a membrane-bound mature BRI2 product. In FBD patients, a point mutation at the stop codon of *BRI2* results in a read-through of the 3′-untranslated region and the synthesis of a BRI2 molecule containing 17 extra amino acids at the C terminus. Furin cleavage generates a longer

Received May 7, 2008; revised June 23, 2008; accepted July 17, 2008.

This work was supported by National Institutes of Health Grants NIA R01 AG22024 (L.D.), NIA R01 AG21588 (L.D.), NIA R21 AG027139 (L.D.), and NIA R01 AG022595 (E.M.M.); American Health Assistance Foundation Grant A2003-076 (L.D.); and Alzheimer's Association Grant IIRG-05-14511 (L.D.). We thank Eric Snapp, J. Kelly Ganjei, Richard Weldon, and Mark Girvin for critical reading of this manuscript.

*S.M. and L.G. contributed equally to this work.

L.D. and L.G. are inventors on a patent owned by the Albert Einstein College of Medicine on the Bri2 KO mice and Bri2 transgenic mice.

Correspondence should be addressed to Luciano D'Adamio, Albert Einstein College of Medicine, Department of Microbiology and Immunology, 1300 Morris Park Avenue, Bronx, NY 10461. E-mail: ldadamio@aecom.yu.edu.

L. Giliberto's present address: Department of Neuroscience, Ophthalmology and Genetics, University of Genova, Via De Toni 5, 16132 Genova, Italy.

DOI:10.1523/JNEUROSCI.2094-08.2008

 0270-6474/08/288668-09$15.00/0

peptide, the ABri peptide, which is deposited as amyloid fibrils. In the Danish kindred, the presence of a 10 nt duplication one codon before the normal stop codon produces a frameshift in the BRI2 sequence generating a larger-than-normal precursor protein, of which the amyloid subunit comprises the last 34 C-terminal amino acids. The role played by *BRI2* mutation in AD-like familial dementias, has prompted us to study the physiological and pathological relevance of the BRI2–APP interaction.

Materials and Methods

Cell culture, transfection, plasmids, and antibodies. Cell lines, transfection methods, human APP, and FLAG-human BRI2 were described previously (Matsuda et al., 2005). γ30 cells, a CHO cell line expressing human APP, human PS1, Aph1-hemagglutinin (HA), and FLAG-Pen2 (Chyung et al., 2005), were kindly provided by Dr. Dennis Selkoe (Center for Neurologic Diseases, Brigham and Women's Hospital and Harvard Medical School, Boston, MA).

pcDNA6-myc-BRI2 was constructed by adding a myc linker at the N terminus of BRI2 (adding MGEQKLISEEDLVPGSA before the initiating methionine of BRI2). Mouse BACE1 was amplified from mouse brain RNA by reverse transcription (RT)-PCR, and cloned into pcDNA3.1/Myc-His(−)B (Invitrogen) to add a C-terminal myc tag. Myc-tagged Notch1 and NotchΔE were described previously (Roncarati et al., 2002). Human APLP1 and APLP2 were cloned in pcDNA3.1/Hygro, and the 20 or 33 aa ectodomain region was replaced with the counterparts of APP by PCR. To construct APP-like protein (APLP)-APP chimeras, either 20 or 33 aa in the ectodomains of APLP1 (RKVNASVPRGFPFHSSEIQR or RKVNASVPRGFPFHSSEIQRDELAPAGTGVSRE) or APLP2 (VKEMIFNAERVGGLEEERES or VKEMIFNAERVGGLEEERESVGPLREDFSLSSS) were replaced with EVKMDAEFRHDSGYEVHHQK or EVKMDAEFRHDSGYEVHHQKLVFFAEDVGSNK of APP. C99 was constructed on pcDNA3.1/Hygro (Invitrogen) so that the human APP leader sequence (MLPGLALLLLAAWTARAL) was fused directly to C-terminal 99 aa of APP. Human Nicastrin cDNA (Open Biosystems; GenBank accession number BC047621) was modified by PCR to remove nucleotides 167–306 and to insert glycine and a HA-tag (GYPYDVPDYA) just before the stop codon. The final construct (hNCT-HA) is identical to C-terminally HA-tagged Nicastrin (GenBank accession number NM_015331). To construct short hairpin RNA (shRNA) vectors, oligonucleotides pairs were annealed and cloned into a modified pSUPER (Zazzeroni et al., 2003), which is driven by H1 promoter. Oligonucleotide pairs used are as follows: sh5 (5′-gatccccgcacatggttattactgatttcaagagaatcagtaataaccatgtgcttttt-3′ and 5′-agctaaaaagcacatggttattactgattctcttgaaatcagtaataaccatgtgcggg-3′), sh10 (5′-gatccccggtgttggtgcatgtgcttttcaagagaaagcacatgcaccaacaccttttt-3′ and 5′-agctaaaaaggtgttggtgcatgtgctttctcttgaaaagcacatgcaccaacaccggg-3′), and m1 (5′-gatccccgcacatgattattactgatttcaagagaatcagtaataatcatgtgctttt-3′ and 5′-agctaaaaagcacatgattattactgattctcttgaaatcagtaataatcatgtgcggg-3′).

The following antibodies and antibody beads were used: αAPP (22C11; Millipore Bioscience Research Reagents; MAB348), αsAPPα (IBL 11088), αAPP C-terminal fragments (CTFs) (Invitrogen/Zymed; 36-6900), αAβ (6E10; Covance; 9300-02; 4G8; Covance; 9200-02), αNicastrin (Cell Signaling Technology; 3632), αhuman PS1 (Millipore Bioscience Research Reagents; MAB1563), αHA (Roche Diagnostics; 3F10), αAPLP1 (EMD/Calbiochem; 171615), and αAPLP2 (Calbiochem; 171616). Antibodies-coupled beads used were as follows: FLAG M2 beads (Sigma-Aldrich; A2220), HA beads (Sigma-Aldrich; A2095), and myc beads (Sigma-Aldrich; A7470). Rabbit polyclonal was from Southern Biotechnology. BRI2 antibody (recognizing amino acids 7–21 of human BRI2) was a generous gift from Dr. Haruhiko Akiyama (Tokyo Institute of Psychiatry, Tokyo, Japan) (Akiyama et al., 2004).

Immunoprecipitations. Cells were transfected with indicated combinations of BACE, APP, APLP1, APLP2, APLPs-APP chimeras, Notch1, NotchΔE, hNCT-HA, FLAG-BRI2, and C99. One day after the transfection, the HeLa cells were lysed in Triton buffer (20 mM HEPES/NaOH, pH 7.4, 1 mM EDTA, 300 mM NaCl, 1% Triton X-100), whereas the γ30 were lysed in HEPES–3-[(3-cholamidopropyl)dimethylammonio]-2-hydroxy-1-propanesulfonate (CHAPSO) buffer (20 mM HEPES/NaOH, pH 7.4, 1 mM EDTA, 150 mM NaCl, 1% CHAPSO). The lysates were cleared by centrifuging at 20,000 × *g* for 10 min. The cleared lysates were mixed with αAPPct and protein A beads for C99 precipitation, with FLAG beads for BRI2 or Pen2 precipitation, or with αHA beads for Nicastrin immunoprecipitation (IP). After being washed four times with Triton buffer, the precipitated beads were boiled in 2× SDS buffer and analyzed by Western blot (WB).

In experiments in which sAPP fragments were analyzed, 1 d after the transfection, the cells were conditioned in 1 ml of medium. On the next day, the medium was collected and cleared by spinning at 20,000 × *g* for 10 min. Cleared samples were analyzed on WB.

Deglycosylation. To deglycosylate the samples, after the SDS samples were completely denatured, aliquots of total lysates and precipitants were incubated with Endo H or PNGase F (New England Biolabs) at 37°C for 2 h. All samples were further analyzed by WB.

Notch1 intracellular domain detection in γ30 cells. γ30 cells were transfected with NotchΔE and FLAG-BRI2. One day after the transfection, the cells were directly lysed in 1× SDS buffer to collect the total lysates that were sonicated to shear the nuclear DNA.

shRNA transfection and Aβ ELISA in HEK293APP cells. The cloned shRNA vectors were transfected into HEK293APP cells. Two days after the transfection, total mRNA was prepared from the transfected cells and untransfected cells with RNeasy mini kit (QIAGEN). The RNA was reverse transcribed with Superscript III (Invitrogen) with random hexamers, and quantitative PCR analysis was performed with pairs of primers (β-actin, 5′-aaggccaaccgcgagaagat-3′ and 5′-tatccctgtacgcctctgg-3′; BRI2, 5′-gtgctatgtgatccctctgaaca-3′ and 5′-tggaacctatttgcctcagtcc-3′) using a SYBR GREEN PCR Master Mix (Applied Biosystems) and ABI PRISM 7900HT Sequence Detection System.

Two days after the transfection, the cells were conditioned for 24 h, and Aβ in the medium was measured using the ELISA kit for Aβ40 and Aβ42 (IBL 17713 and 17711, respectively). Cells were lysed in RIPA buffer and equal amounts of proteins were analyzed by WB.

Mouse brain preparations for WB and ELISA. A total of 100 mg of mouse brains was homogenized in 1 ml of HEPES–sucrose buffer (20 mM HEPES/NaOH, pH 7.4, 1 mM EDTA, 1 mM EGTA, 0.25 M sucrose) supplemented with protease inhibitors (PIs). The PNS was prepared by precipitating the nuclei and debris by centrifuging the homogenates at 1000 × *g* for 10 min. Twenty micrograms of each PNS were loaded by SDS-PAGE.

Aβ was extracted from the homogenates by formic acid. A total of 200 μl of the above homogenates was mixed with 440 μl of formic acid and sonicated on ice for 1 min. A total of 400 μl of the sonicated homogenate was cleared by centrifuging at 100,000 × *g* for 45 min. A total of 210 μl of the cleared supernatant was neutralized with 4 ml of neutralization buffer (1 M Tris base, 0.5 M Na_2HPO_4, 0.05% NaN_3, pH not adjusted). The extracted Aβ was measured with the ELISA kits described above. sAPPα and sAPPβ were measured by ELISA (IBL 11088 and 10321, respectively) using brain PNS.

To prepare mouse brain membrane, PNS was precipitated by centrifuging at 100,000 × *g* for 45 min, and the precipitated membrane was suspended in HEPES–sucrose buffer. Equal amount of proteins were used for WB.

For IP, after precipitating the membrane by centrifuging at 100,000 × *g*, membrane was extracted with HEPES–Triton buffer (20 mM HEPES/NaOH, pH 7.4, 1 mM EDTA, 150 mM NaCl, 0.5% Triton X-100) containing 10% glycerol supplemented with PIs. Extracts were cleared by centrifuging at 100,000 × *g* for 45 min, and were precleared with protein A beads (Pierce). Precleared extracts were mixed with αBRI2, αAPPct, or control rabbit polyclonal antibodies, and antibody complex was precipitated with protein A beads. After being washed four times with HEPES–Triton buffer, the precipitants were boiled in 2× SDS buffer and were analyzed by WB.

Generation of human BRI2 *transgenic mice and of* $Bri2^{-/-}$ *mice.* Generation of human *BRI2* transgenic mice and of $Bri2^{-/-}$ mice is described in supplemental Figures S1 and S3 (available at www.jneurosci.org as supplemental material).

Other mouse transgenic lines. In the BRI2tg mouse, human *BRI2* is expressed under the control of the mouse prion promoter (Pickford et al., 2006). CRND8 mice (Chishti et al., 2001) carry a double mutation of

APP695: KM595/596/NL (Swedish mutation), and V642F (Indiana mutation). The transgene is under the control of Syrian hamster prion promoter. B6C3-Tg (APPswe, PSEN1ΔE9) 85Dbo/J mice were purchased from The Jackson Laboratory (Savonenko et al., 2003). This is a double transgenic mouse expressing a chimeric mouse/human amyloid precursor protein (Mo/HuAPP695swe) and a mutant human Presenilin 1 (PS1ΔE9) under the control of the Syrian hamster prion promoter. Both mutations are associated with early-onset AD. These mice secrete human Aβ peptides and develop β-amyloid deposits in the brains by 6–7 months of age.

Mouse brain dissection and processing for immunohistochemistry and amyloid plaque burden determination. Details for these procedures are discussed in supplemental Figure S2 (available at www.jneurosci.org as supplemental material).

Mouse handling. BRI28.4 and 5.5 mice were maintained on a FVB background; BRI2 Tg mice were maintained on a Swiss Webster background; CRND8 and APP/PS1 mice were maintained on a C57BL/6 background. Mice were handled according to the Ethical Guidelines for Treatment of Laboratory Animals of Albert Einstein College of Medicine. The procedures were described and approved in animal protocol number 20040707.

Image scanning and analysis. WB images were scanned with Epson perfection 3200 Photo scanner and were analyzed with NIH Image software.

Statistical analysis. All quantified data represent an average of at least triplicate samples. Error bars represent SEMs. Statistical significance was determined by Student's *t* test, and a value of $p < 0.05$ was considered significant.

Results

BRI2 is a physiological inhibitor of APP processing

BRI2 was hit on while screening for transmembrane proteins that bind APP and inhibits its processing (Matsuda et al., 2005). Inhibition of APP processing by BRI2 may represent an artifact of overexpression rather than reflect the physiological function of BRI2. To address this issue, we downregulated endogenous BRI2 by RNA interference (RNAi) using shRNAs corresponding to human BRI2 (sh5 and sh10) or a point mutant of sh5 (m1). Quantitative PCR showed that sh5 and sh10 reduced the *BRI2* mRNA levels to <10% of the levels found in untransfected cells, whereas m1 modestly reduced the *BRI2* mRNA levels (Fig. 1*A*). These data were confirmed by WB analysis, which shows reduced levels of BRI2 in the sh5 and sh10 transfected cells (Fig. 1*B*). The reduction was specific because the levels of APP and tubulin were not changed (Fig. 1*B*). To determine whether lowering BRI2 expression has any impact on APP processing, we measured the levels of sAPPα, sAPPβ, and Aβ peptides in the conditioned media of HEK293APP cells and found that BRI2 downregulation significantly augmented sAPPα, sAPPβ, Aβ40, and Aβ42 levels (Fig. 1*B*,*C*). Thus, whereas BRI2 overexpression reduces APP cleavage, depletion of BRI2 levels has the opposite effect and leads to increased levels of Aβ peptides. These results suggest that BRI2 is a physiological inhibitor of APP processing and Aβ production.

Next, we generated *Bri2*-null mice that provide an excellent animal model to validate the role of BRI2 in APP processing (supplemental Fig. S3*A*, available at www.jneurosci.org as supplemental material). To determine how deletion of exon 2 impacts Bri2 protein expression, we performed WB analysis on brain lysates from wild-type (wt), Bri2 $^{-/-}$, and Bri2 $^{+/-}$ APP $^{-/-}$ mice. As expected, Bri2 $^{-/-}$ animals did not express Bri2 protein, which is readily detectable in wild-type mice. Also, Bri2 $^{+/-}$ animals expressed lower levels of Bri2 (Fig. 2*A*). Analysis of wild-type, Bri2 $^{-/-}$, and APP $^{-/-}$ mice showed lack of Bri2 expression does not impact on the levels of APP protein and vice versa. Of note, IP of brain lysates with the αBri2 antibody shows that mAPP is bound to APP only in wild-type animals, but not in Bri2 $^{-/-}$ and APP $^{-/-}$ (Fig. 2*B*).

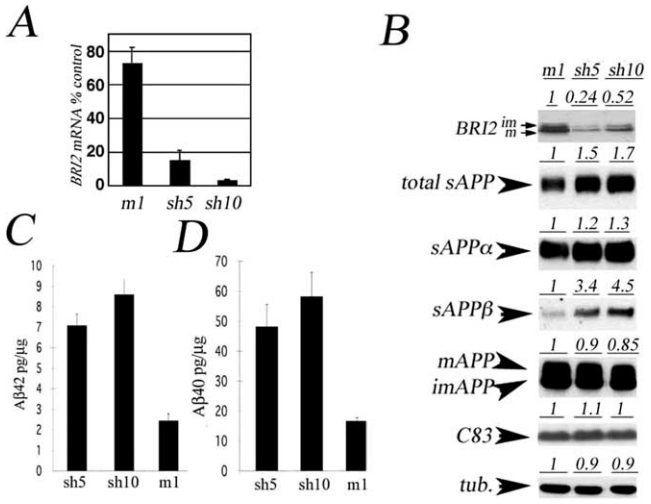

Figure 1. BRI2 is a physiological inhibitor of Aβ generation in cell lines. ***A***, RNAi-mediated reduction of BRI2 expression with BRI2-specific short hairpin constructs sh5 and sh10 in HEK293APP cells. Interference was verified by real-time quantitative RT-PCR. Quantitative PCR analysis of BRI2 mRNA of HEK293APP cells transfected with control (m1) or BRI2 shRNAs (sh5 and sh10). The abundance of BRI2 mRNA is normalized by that of β-actin, and is displayed as a percentage of normalized BRI2 mRNA of untransfected cells. ***B***, WB of the same samples indicates the reduction of both mature (m) and immature (im) BRI2 in cells transfected with BRI2 shRNAs. Also, whereas α-tubulin, mAPP, imAPP, and C83 levels are similar in all samples, sAPPα and sAPPβ are increased by sh5 and sh10. The numbers above the WBs indicate the relative amounts of proteins detected. The amount present in the M1 sample was given an arbitrary value of 1. ***C***, ***D***, Aβ ELISA from supernatants of HEK293APP cells shows that reducing BRI2 expression results in increased Aβ40 and Aβ42 production. Error bars indicate SEM.

Bri2 $^{-/-}$ mice are viable and fertile with no obvious changes in overall APP levels (Fig. 2*C*). Analysis of 11-month-old *Bri2* $^{-/-}$ mice and wt littermates as control for APP processing in brain showed statistically significant increase in both endogenous sAPPα and sAPPβ levels (Fig. 2*C*,*D*). Next, *Bri2* $^{+/-}$ mice were crossed to TgAPP695/PSEN1DE9 double transgenic mice (called here *APP-PS1*) expressing two familial Alzheimer's disease mutant genes (APP-Swedish and PS1ΔE9) (Savonenko et al., 2003). We analyzed two 8-month-old and one 4-month-old *Bri2* $^{+/-}$/*APP-PS1* mice. These mice were compared with age-matched *Bri2* $^{+/+}$/*APP-PS1*. We observed an obvious increase in sAPPα production in brain homogenates of *Bri2* $^{+/-}$/*APP-PS1* compared with *Bri2* $^{+/+}$/*APP-PS1* controls (Fig. 3). WB analysis showed that Aβ is visible only in the 8-month-old mice and those *Bri2* heterozygous mice present significantly higher levels of Aβ peptides than wild-type BRI2 animals (Fig. 3). To better quantify levels of Aβ40 and Aβ42, we analyzed brain extracts by ELISA. Given the better sensitivity, this assay detected Aβ in the 4-month-old mouse samples as well. These measurements confirmed a statistically significant increase of both Aβ40 and Aβ42 in *Bri2* $^{+/-}$ compared with *Bri2* $^{+/+}$ mice (data not shown). Thus, halving Bri2 expression by gene targeting increases APP processing and Aβ formation.

BRI2 does not affect the activity of secretases

Next, we studied the mechanisms by which BRI2 interferes with APP processing. First, we addressed whether BRI2 inhibits the activity of secretases. To this end, we initially tested whether BRI2 physically interacts with γ- and/or β-secretase and found that

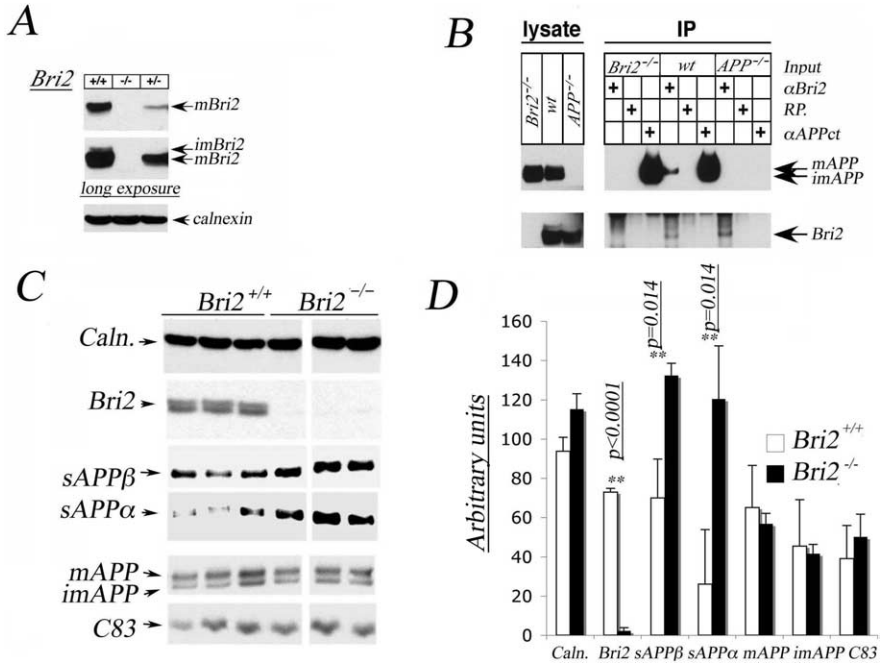

Figure 2. BRI2 is a physiological inhibitor of APP processing and Aβ generation in the mouse brain. ***A***, WB analysis of brain membranes from *Bri2* $^{+/+}$, *Bri2* $^{+/-}$, and *Bri2* $^{-/-}$ mice shows lack or reduced levels of Bri2 expression in *Bri2* $^{-/-}$ and *Bri2* $^{+/-}$ mice, respectively. Calnexin is used as a control to verify equal loading of protein samples. ***B***, Analysis of brain membrane extracts from *Bri2* $^{-/-}$ and *APP* $^{-/-}$ mice. Total lysates were analyzed for Bri2 and APP expression (left panel). Brain lysates were immunoprecipitated with the αBRI2, αAPPct, and rabbit polyclonal (RP) control antibody (right panel). Precipitates were analyzed for APP and Bri2 proteins. *Bri2* $^{-/-}$ and wild-type mice express equal amounts of APP. IP of endogenous APP with the αBRI2 antibody is specific because APP is precipitated in wild-type mice but neither *APP* $^{-/-}$ nor *Bri2* $^{-/-}$ mice. ***C***, The brains of six 11-month-old male Bri2 $^{-/-}$ and wt littermates were analyzed for APP-derived fragments in the brain. Calnexin (Caln.) is used as a control to verify equal loading of protein samples. ***D***, Quantification of the WBs shown in ***C***. The increases in sAPPβ and -sAPPα observed in Bri2 $^{-/-}$ mice are statistically significant when compared with wt littermates. Error bars indicate SEM.

BRI2 does not bind those secretases (Fig. 4*A*,*B*). Second, we tested whether BRI2 regulates processing of three other substrates of secretases. Two, APLP1 and APLP2, were selected because they are structurally similar to APP and are processed by γ-, α-, and β-secretases in the same way (Scheinfeld et al., 2002; Li and Südhof, 2004). The third, Notch1, is, together with APP, the best characterized γ-secretase substrate because its cleavage generates the intracellular domain [Notch1 intracellular domain (NICD)] that regulates transcription of genes important for neuronal development, synapse formation, cell death, etc. (Annaert and De Strooper, 1999; Artavanis-Tsakonas et al., 1999; Sestan et al., 1999). Four APLP1/2 polypeptides are visible in transfected cells: mAPLP1/2, imAPLP1/2, as well as C-terminal fragments derived from either α- or β-secretase cleavage (α-CTF and β-CTF, respectively) (Fig. 4*D*,*E*). BRI2 binds neither APLP1 nor APLP2 and it does not alter their processing because the levels of α-CTF and β-CTF are unchanged (Fig. 4*D*,*E*). Similar data were obtained for Notch1; BRI2 does not interact with Notch1 or the Notch1-derived γ-secretase substrate NotchΔE (Fig. 4*F*). In addition, it does not inhibit γ-cleavage of NotchΔE (Fig. 4*G*).

By binding APP, BRI2 interferes with α/β-secretase cleavage and docking of the γ-secretase to APP

Thus, two lines of evidence suggest that BRI2 serves as a competitive inhibitor of processing that limits access of secretases to APP. First, the region of APP comprised between the β- and α-secretase cleavage sites is essential for the mBRI2–mAPP interaction. Second, BRI2 does not interfere with processing of other substrates of secretases. However, these hypotheses cannot be tested directly because the physical interaction of APP and β-secretase cannot be detected and the molecular identity of the α-secretase is still elusive. Thus, we approached this question indirectly, inserting extracellular APP regions comprising the β- and α-cleavage sites into either APLP1 or APLP2. Two sets of chimeric APLPs-APP molecules were made, which included either amino acids 593–612 or 593–625 of APP (called APLP1/2-APP[20] and APLP1/2-APP[33], respectively) (Fig. 5*A*). If our model is correct, processing of APLP-APP chimeras that bind BRI2 should be reduced by BRI2. As shown in Figure 4*B*, APLP1-APP[33] and APLP2-APP[33] chimeras interacted with BRI2, whereas APLP1-APP[20] and APLP2-APP[20] did not. Notably, and as for APP, BRI2 interacted with and stabilized the β-CTF fragment derived from β-cleavage of either APLP1-APP[33] or APLP2-APP[33] but not APLP1-APP[20] or APLP2-APP[20] (Fig. 5*B*). Thus, the 593–625 region of APP is sufficient for BRI2 binding and for transferring the inhibitory activity of BRI2 on γ-processing. To test whether BRI2 also inhibited β- and α-cleavage of APLP1-APP[33] and APLP2-APP[33] chimeras, we measured sAPLP1/2-APPα and sAPLP1/2-APPβ in the supernatant of transfected cell cultures. Production of sAPLP1-APPα, sAPLP2-APPα, and sAPLP1-APPβ was clearly reduced by BRI2 (sAPLP2-APPβ was undetectable even in the control sample) (data not shown). Together, these data indicate that BRI2 inhibits α- and β-cleavage of APLP1-APP[33] and APLP2-APP[33] chimeras as well as γ-processing of the corresponding β-CTF fragments.

The cytoplasmic tail of APP binds several intracellular adaptor proteins and the sequences surrounding Tyr[682] and Thr[668] are required for binding. Most of these proteins also bind APLP1 and APLP2 (Minopoli et al., 2006). To test whether the effect of BRI2 on processing of APP, APLP1-APP[33], and APLP2-APP[33] chimeras was attributable to interferences with intracellular adaptor proteins binding and/or function, we tested APP$^{\Delta C31}$, which is missing the cytoplasmic sequences required for binding to adaptor proteins. As evident in Figure 5*D*, BRI2 binds APP$^{\Delta C31}$ and inhibits its processing. Thus, BRI2 does not regulate APP processing indirectly, modulating the function of intracellular adaptor of APP.

Hence BRI2 inhibits APP processing by masking the β- and α-secretase cleavage sites. But because the intramembranous region of APP is not involved in BRI2 binding, the γ-secretase cleavage sites should not be concealed by BRI2. The substrate recognition subunit of γ-secretase NCT, however, binds the extracellular segment of C99, where also BRI2 interacts (Yu et al., 2000; De Strooper, 2005; Shah et al., 2005). Thus, we tested whether BRI2 and NCT compete for binding to BRI2. C99 binds both mature and immature forms of NCT in transfected cells (Fig. 5*E*). The interaction with mNCT reflects the biologically relevant docking of γ-secretase to C99 (Shah et al., 2005). Importantly, BRI2 reduced the interaction of C99 with mNCT, whereas it did not impact the C99/imNCT association

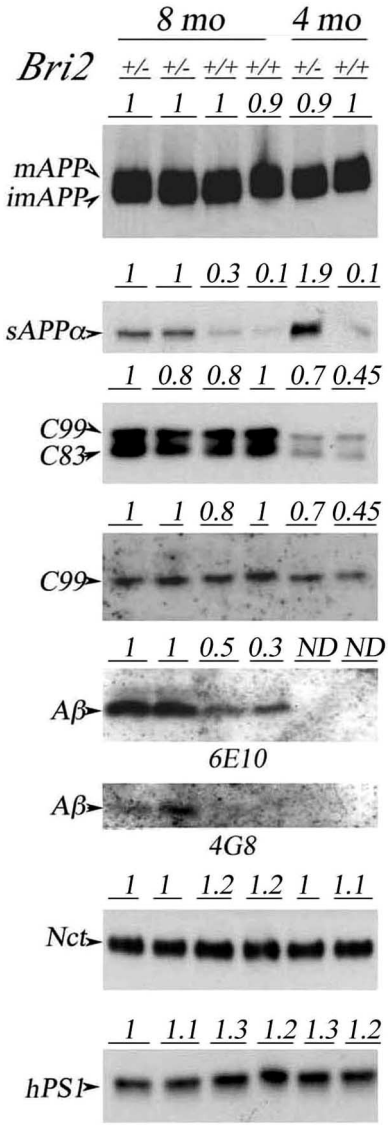

Figure 3. Reducing BRI2 levels increases processing of a FAD APP mutant *in vivo*. *Bri2* $^{+/-}$ mice were crossed to *APP-PS1* tag APP and PS1 mutant transgenic mice to obtain *Bri2* $^{+/-}$/*APP-PS1* and *Bri2* $^{+/+}$/*APP-PS1* animals. WB analysis of postnuclear supernatants of 8-month-old (2 *Bri2* $^{+/-}$/*APP-PS1* and 2 *Bri2* $^{+/+}$/*APP-PS1*) and 4-month-old (1 *Bri2* $^{+/-}$/*APP-PS1* and 1 *Bri2* $^{+/+}$/*APP-PS1*) shows the following: total APP (mouse plus transgenic human APP), C83, C99, Nct, and human PS1DE9 levels are similar among mice in each age group. However, sAPPα is increased in the *Bri2* $^{+/-}$/*APP-PS1* mice compared with the *Bri2* $^{+/+}$/*APP-PS1* littermates. As for total Aβ, the peptide is only detectable in 8-month-old mice. Interestingly, total Aβ is increased in the two *Bri2* $^{+/-}$/*APP-PS1*. Aβ is detected by two different monoclonal antibodies, 6E10 and 4G8. The numbers above the WBs indicate the relative amounts of proteins detected. The amount present in the first Bri2 $^{+/+}$ sample was given an arbitrary value of 1.

(Fig. 5*E*,*G*). The reverse experiment showed similar results. NCT copurified C99 and BRI2 reduced the levels of C99–NCT complexes (Fig. 5*F*). These results indicate that BRI2 inhibits docking of γ-secretase to C99.

BRI2 reduces AD pathology

Next, we tested whether BRI2 can reduce APP processing and AD pathology *in vivo*. To this end, we generated transgenic mice expressing human wild-type *BRI2* under the control of the αCaMKII promoter (S1A). The αCaMKII promoter was chosen because it drives the expression of transgenes in the postnatal forebrain (Mayford et al., 1996), which is the area markedly affected by AD. This selective spatiotemporal expression reduces issues arising from expression of the transgene during development or in other organs and tissues. Two *BRI2tg* mouse lines, BRI2-8.4 and BRI2-5.5, that expressed distinct levels of transgenic BRI2 (Fig. 6*A*) were further analyzed. First, we analyzed APP processing in 2-month-old BRI2-8.4 transgenic mice and littermate controls. As shown in Figure 6*B*, transgenic expression of BRI2 correlated with decreases amounts of sAPPβ and total sAPP fragments. Then, BRI2-8.4 and BRI2-5.5 were crossed to CRND8 mice, a well characterized mouse model of AD expressing a mutant human APP transgene (Chishti et al., 2001). CRND8 mice develop Aβ-containing amyloid plaques at 3 months of age. We also used another transgenic model in which the mouse prion promoter drives *BRI2* expression (Pickford et al., 2006). This promoter has a similar expression pattern to the hamster prion promoter controlling *APP* expression in the CRND8 mice. In this model, human APP and BRI2 are coexpressed in a spatiotemporal manner. CRND8/BRI2 double-transgenic mice and CRND8 single-transgenic littermates were analyzed for sAPPα, sAPPβ, and amyloid plaque levels. Mice were killed at the indicated ages, and brains were isolated. Of importance, transgenic BRI2 expression did not change the levels of transgenic hAPP protein (data not shown). Yet, double-transgenic mice had significantly reduced sAPPα, sAPPβ, Aβ40, and Aβ42 levels compared with littermate CRND8 controls. Total brain Aβ40, Aβ42, sAPPα, and sAPPβ were analyzed by ELISA at different ages. The α- and β-secretase-derived products sAPPα and sAPPβ were measured in 3-month-old BRI2-8.4/CRND8 female and CRND8 female littermates (three BRI2-8.4/CRND8 and four CRND8; experiment 1), 4-month-old BRI2-5.5/CRND8 and CRND8 littermates (nine CRND8 males and five male BRI2-5.5/CRND8 mice; experiment 2), 6-month-old BRI2/CRND8 and CRND8 littermates (two female and two male CRND8 vs one female and two male BRI2/CRND8 mice; experiment 3). The amounts of sAPP products in the tgBRI2/CRND8 mice is expressed as a percentage of the sAPPs found in the CRND8 mice of the same experimental group, which is assumed to be 100%. We registered the following values: (1) experiment 1: (i) sAPPα, CRND8, 99.6 ± 38 SD, and BRI2-8.4/CRND8, 57.5 ± 26.6 SD ($p = 0.032$); (ii) sAPPβ, CRND8, 100 ± 33.5 SD, and BRI2-8.4/CRND8, 45 ± 19.7 SD ($p = 0.039$); (2) experiment 2: (i) sAPPα, CRND8, 101 ± 34.7 SD, and BRI2-8.4/CRND8, 45.4 ± 13.1 SD ($p = 0.046$); (ii) sAPPβ, CRND8, 100 ± 41 SD, and BRI2-8.4/CRND8, 53 ± 25 SD ($p = 0.04$); (3) experiment 3: (i) sAPPα, CRND8, 100 ± 7.5 SD, and BRI2-8.4/CRND8, 63 ± 16 SD ($p = 0.006$); (ii) sAPPβ, CRND8, 100 ± 11 SD, and BRI2-8.4/CRND8, 65.8 ± 21.7 SD ($p = 0.03$).

Aβ40 and Aβ42 were measured in the 6-month-old BRI2/CRND8 and CRND8 littermates, and we found significant decrease in both peptides ($p = 0.028$ for Aβ42 and $p = 0.02$ for Aβ40). These *in vivo* data are consistent with the result that BRI2 overexpression inhibits both α- and β-secretases, although we cannot exclude the possibility that the *BRI2* transgene also accelerates the catabolism of sAPPα and sAPPβ in mouse brain. Accordingly, transgenic expression of hBRI2 meaningfully decreased amyloid burden in all three mouse lines (Fig. 7). Quantification of amyloid plaque burden present in the brain of the single- and double-transgenic littermate groups showed a reduction in the area occupied by amyloid plaques in the tgBRI2/CRND8 mice compared with CRND8 mice of the same experimental group, which is assumed to be 100%. The following values were recorded: (1) mice, 3 months of age, six female CRND8, 104 ± 16.4 SD, versus two male plus six female BRI2-5.5/

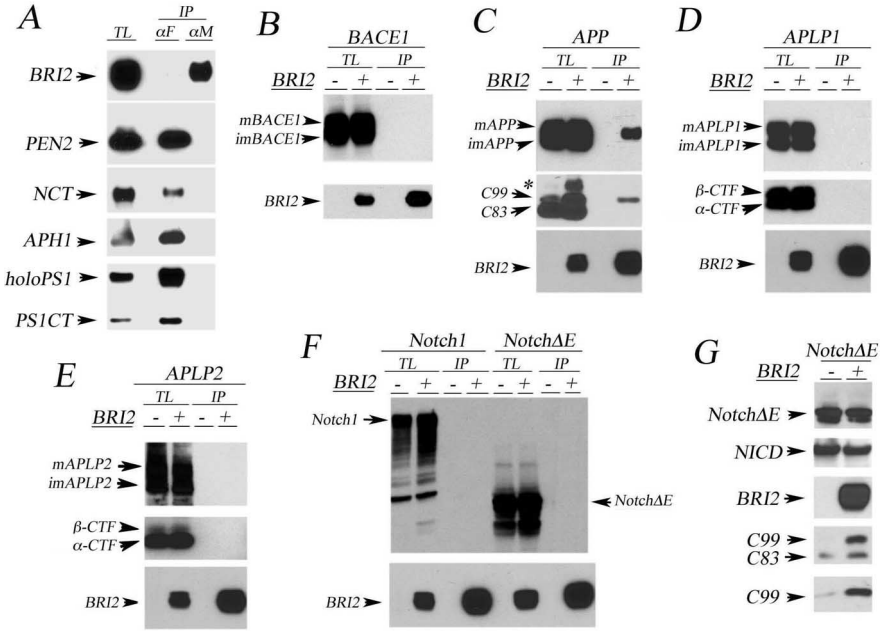

Figure 4. BRI2 is a specific inhibitor of APP processing. ***A***, γ30 cells, which express high levels of endogenous NCT and overexpress the γ-secretase components PS1, Pen2 (Flag-tagged), and Aph1, were transfected with Myc-tagged BRI2. IP of Flag-Pen2 isolates the γ-secretase complex but not BRI2. Conversely, precipitation of Myc-BRI2 did not pull-down any γ-secretase component. TL, Total lysates. ***B***, HeLa cell were transfected with β-secretase (BACE1), with or without BRI2. BRI2 IP does not isolate BACE1. HeLa cells were transfected with APP (***C***), APLP1 (***D***), APLP2 (***E***), Notch1, or NotchΔE (***F***, ***G***) alone or plus FLAG-tagged BRI2. Proteins were immunoprecipitated with a αFLAG antibody and eluted with the FLAG epitope peptide (IP). BRI2 interacts with both mAPP and C99 (***C***) but not APLP1 (or C-terminal APLP1β and APLP1α-stubs), APLP2 (or C-terminal APLP2β and APLP2α-stubs), Notch, or NotchΔE (***D–F***). BRI2 affects APP processing and generation of C99 (***C***), but it does not impact on the levels of APLP1 and APLP2 processing (***D***, ***E***), because the levels of C-terminal stubs are not altered. ***G***, BRI2 does not inhibit cleavage of NotchΔE by γ-secretases and generation of NICD, whereas, in the same transfected cells, it inhibits endogenous APP processing as demonstrated by increased C99 levels. The bottom two panels were probed with either αAPPct (fourth panel from the top), which detects both C83 and C99, or 6E10 (bottom panel), which reacts only with C99.

CRND8, 51.5 ± 13 SD ($p = 0.0001$); (2) 5 months of age, three male plus three female CRND8, 111 ± 14 SD, and one male plus three female BRI2-5.5/CRND8, 72.7 ± 13 SD ($p = 0.0024$); (3) 4 months of age, four female CRND8, 100 ± 18.7 SD, and four female BRI2/CRND8, 24.5 ± 26 SD ($p = 0.0033$); (4) 6 months of age, two male plus four female CRND8, 107 ± 10.7 SD, and five male plus four female BRI2-8.4/CRND8, 65 ± 9 SD ($p = 0.0001$); (5) 7 months of age, three male plus two female CRND8, 93 ± 14 SD, and four male plus three female BRI2-8.4/CRND8, 65 ± 16 SD ($p = 0.006$).

Discussion

Extracellular aggregates of Aβ42, which derives from cleavage of APP, characterize AD pathology. Genetic data support the notion that deregulation of APP processing and Aβ production plays a central role in AD pathogenesis. Indeed, familial forms of AD are caused by mutations in the Aβ precursor APP and in Presenilins, the catalytic components of the γ-secretase, the protease that generates Aβ. APP missense mutations promote the amyloidogenic processing and lead to higher levels of Aβ42. Likewise, FAD-linked PS1 and PS2 mutations selectively enhance Aβ42 production, although total Aβ is in many cases reduced or unchanged. The increase of fibrillogenic Aβ42 has supported the prevailing view that Presenilin mutations cause FAD through a gain-of-function toxic mechanism, very much like the APP mutation.

Despite the central role of APP cleavage in APP signaling and AD pathogenesis, little is known about the molecular mechanisms that regulate the activity of secretases on APP. The type II membrane protein BRI2 was identified during a genetic screen for APP ligands that regulate APP processing (Matsuda et al., 2005). Numerous lines of evidence shown here indicate that BRI2 plays a significant role in APP processing. BRI2 physically associates with APP, and this interaction serves to suppress APP processing by secretases and the production of Aβ *in vivo*. Increasing BRI2 levels in the mouse brain by transgenic expression reduces APP cleavage by α- and β-secretase as well as amyloid plaque formation. However, reducing BRI2 expression in cell lines by RNAi and by gene targeting in mice increases APP processing. In fact, sAPPα, sAPPβ, Aβ40, and Aβ42 levels are increased in BRI2 knockdown cells (Fig. 1). Moreover, sAPPα, sAPPβ, Aβ40, and Aβ42 are also augmented in $Bri2^{+/-}$ and $Bri2^{-/-}$ mice brains, in which Bri2 expression is genetically halved or ablated (Fig. 2). Together, these data demonstrate that BRI2 is an important physiological regulator of α-, β-, and γ-processing of APP. In addition, they hint to the possibility that genetic or environmental factors interfering with the regulation of APP processing by BRI2 may contribute to Alzheimer's disease pathogenesis.

Because BRI2 inhibits cleavage of APP by all three secretases, it seems unlikely that BRI2 functions as an inhibitor of secretases. Also, BRI2 neither interacts with BACE1, γ-secretase, or their substrates Notch, APLP1, and APLP2 nor does it interfere with Notch, APLP1, and APLP2 processing (Fig. 4). Because BRI2 binds the region of APP spanning amino acids 597 (the N terminus of C99) to 625 (the C terminus of APLP1/2-APP[33] chimeras), which includes the β- and α-cleavage sites, it is conceivable that BRI2 masks the β- and α-secretase cleavage sites of APP. This hypothesis is supported by the experiments in Figure 5, *B* and *C*, in which transferring the BRI2-binding motif of APP to either APLP1 or APLP2 generates chimeric molecules that BRI2 binds and protects from processing by secretases. As for γ-secretase, the transmembrane region of APP, in which γ-cleavage sites are, is not directly involved in BRI2 binding. However, the BRI2 interaction domain on C99 also includes the docking site for γ-secretase (Shah et al., 2005), suggesting that BRI2 acts as a competitive inhibitor of γ-secretase binding to C99. In accordance with this model, we found that BRI2 reduces binding of NCT, the docking subunit of the γ-secretase, to C99 (Fig. 4*E–G*). Overall, our data indicate that BRI2 masks the cleavage sites of β- and α-secretase on APP and the γ-secretase docking site on C99. This mechanism of inhibition of amyloid formation by BRI2 suggests an alternative therapeutic approach to AD aimed at inhibiting access of secretases to APP rather than the activity of secretases. This method would avoid toxic effects caused by inhibiting processing of other substrates of secretases (Evin et al., 2006) or even a direct pathogenic effect of γ-secretase inhibitors, as postulated by others (Saura et al., 2004; Shen and Kelleher, 2007). These findings raise the valid concern

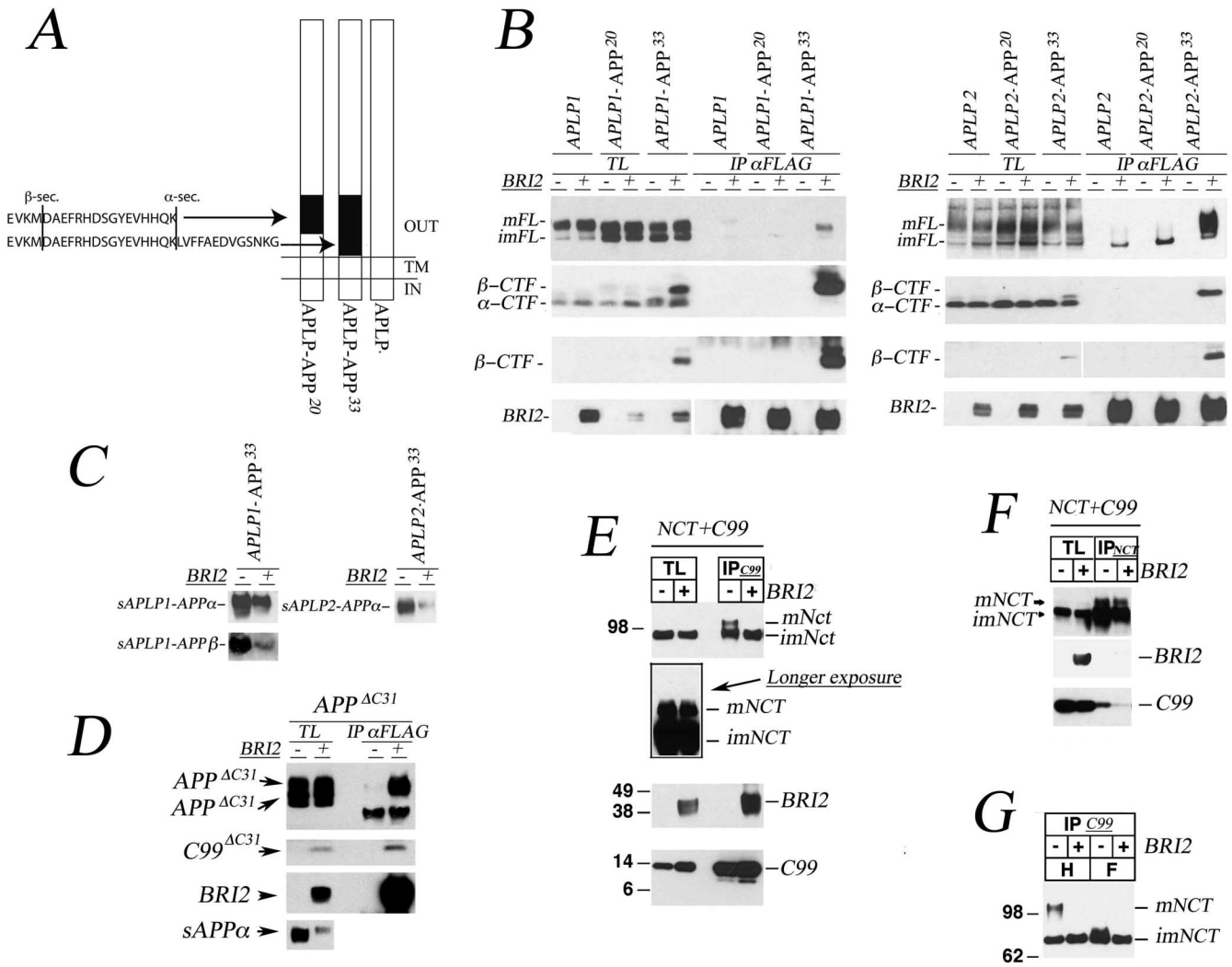

Figure 5. BRI2 masks the α- and β-secretase cleavage sites of APP and competes with NCT for binding to C99. ***A***, Schematic representation of APLP1/2-APP ^{20} APLP1/2-APP ^{33} chimeric molecule. The sequences on the far left represent the APP regions inserted in APLP molecules for the APLP1/2-APP ^{20} (top sequence) and APLP1/2-APP ^{33} (bottom sequence) chimeras. The α- and β-cleavage sites are indicated. TM, Transmembrane. ***B***, HeLa cells were transfected with the indicated APLPs-APP constructs, with or without FLAG-BRI2. Total lysates (TL) and αFLAG-immunoprecipitates were analyzed by WB. mAPLP1-APP ^{33} and mAPLP2-APP ^{33} chimeras bind BRI2 and BRI2 increases the β-CTF produced by mAPLP1-APP ^{33} and mAPLP2-APP ^{33}. ***C***, Analysis of supernatants derived from transfected HeLa cells shows that BRI2 inhibits production of sAPLP1-APPα, sAPLP1-APPβ, and sAPLP2-APPα. ***D***, HeLa cells were transfected with the APPΔC31 construct, with or without FLAG-BRI2. Total lysates (TL), αFLAG-immunoprecipitates, and cell culture supernatants were analyzed as in ***B*** and ***C***. mAPPΔC31 binds BRI2, and BRI2 increases C99ΔC31, whereas it inhibits production of sAPPα (APPβ was not detected) (data not shown). ***E***, HeLa cells were transfected with C99 and NCT. Two NCT bands are visible: the bottom band is the predominant specie present in total lysates, whereas the top band is visible only after longer exposure (second panel). IP of C99 isolates both NCT species but enriches for the higher molecular weight form. When BRI2 is coexpressed, C99 preferentially interacts with BRI2 over mNCT. ***F***, Reverse IP shows that NCT coprecipitates C99. BRI2 expression reduces the amount of C99 bound to NCT, and NCT does not copurify BRI2. ***G***, EndoH (H) and PNGase F (F) digestion of C99 immunoprecipitates shows that the top NCT form represents mature NCT because it is resistant to endoH digestion but sensitive to PNGase F, whereas the bottom molecular species is immature NCT. Again, expression of BRI2 inhibits the interaction between C99 and mNCT.

that γ-secretase inhibitors may be pathogenic rather than therapeutic and accelerate the development of Alzheimer's disease.

A study published while we were revising our manuscript indicates that the Bri2-23 peptide released from the BRI2 protein by furin/furin-like protease cleavage can inhibit Aβ aggregation *in vitro* and that overexpression of BRI2 reduced Aβ deposition in APP CRND8 mice (Kim et al., 2008). Thus, BRI2 may influence both Aβ formation and deposition phenotype in multiple ways.

Interestingly, *BRI2* mutations are associated with familial British and Danish dementias (Vidal et al., 1999, 2000), two autosomal dominant neurodegenerative disorders characterized by parenchymal amyloid deposits and extensive cerebral amyloid angiopathy (Revesz et al., 2002). The finding that the familial dementia gene *BRI2* functionally interacts with the dementia gene *APP*, thereby regulating a biochemical event central to the pathogenesis of Alzheimer's disease, sparks the question of whether BRI2 and APP pathogenic mutations alter these regulatory mechanisms.

References

Akiyama H, Kondo H, Arai T, Ikeda K, Kato M, Iseki E, Schwab C, McGeer PL (2004) Expression of BRI, the normal precursor of the amyloid protein of familial British dementia, in human brain. Acta Neuropathol 107:53–58.

Annaert W, De Strooper B (1999) Presenilins: molecular switches between proteolysis and signal transduction. Trends Neurosci 22:439–443.

Artavanis-Tsakonas S, Rand MD, Lake RJ (1999) Notch signaling: cell fate control and signal integration in development. Science 284:770–776.

Breteler MM, Claus JJ, van Duijn CM, Launer LJ, Hofman A (1992) Epidemiology of Alzheimer's disease. Epidemiol Rev 14:59–82.

Cao X, Südhof TC (2001) A transcriptionally [correction of transcriptively] active complex of APP with Fe65 and histone acetyltransferase Tip60. Science 293:115–120.

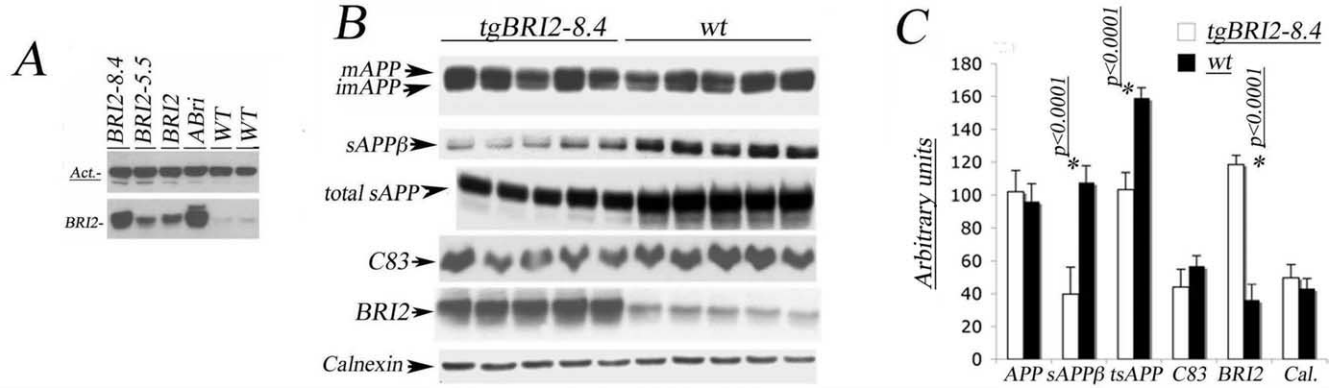

Figure 6. BRI2 overexpression inhibits APP processing in normal animals and APP mutant transgenic mice. ***A***, WBs of two wild-type animals and the progeny of lines BRI2-8.4, BRI2-8.5, BRI2, and ABri (Pickford et al., 2006) with the αBRI2 antibody indicate that the BRI2 protein is overexpressed in tgBRI2 animals. ***B***, WBs of five BRI2-8.4 transgenic mice and wild-type littermates (mice were all 2-month-old males) show that (1) overexpression of BRI2 does not appreciably affect the total levels of APP or the mAPP:imAPP ratio in the brain; (2) the levels of C83 are not consistently changed (the levels of C99/89 are below detection); (3) BRI2 overexpression reduces the levels of sAPPβ and sAPPβ-sAPPα (total sAPP, detected by 22C11 in the soluble protein fraction, which is deprived of full-length APP). Calnexin is used as an internal control for protein loading. ***C***, Quantification of the WBs shown in ***B***. The decreases in sAPPβ and total-sAPP (tsAPP) as well as the increase in BRI2 observed in tgBRI2-8.4 mice are statistically significant when compared with wt littermates. Cal., Calnexin. Error bars indicate SEM.

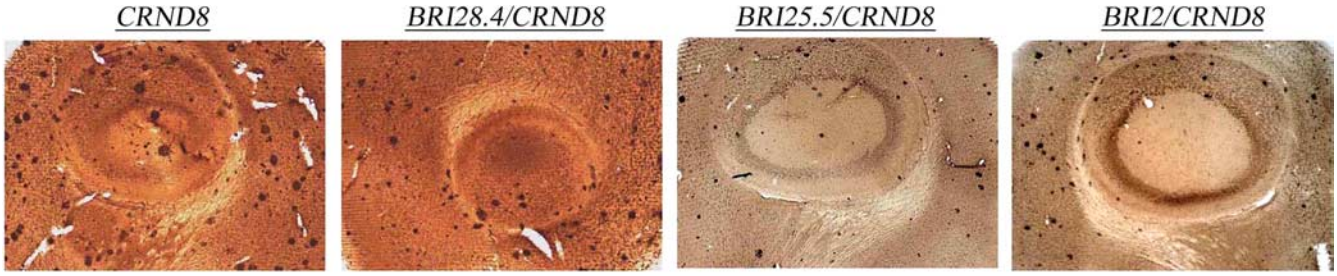

Figure 7. BRI2 reduces AD pathology in APP mutant transgenic mice. Cortical sections of 6-month-old mice stained with αAβ 6E10 show a reduction in amyloid pathology in BRI2 transgenic-CRND8 mice.

Chishti MA, Yang DS, Janus C, Phinney AL, Horne P, Pearson J, Strome R, Zuker N, Loukides J, French J, Turner S, Lozza G, Grilli M, Kunicki S, Morissette C, Paquette J, Gervais F, Bergeron C, Fraser PE, Carlson GA, et al. (2001) Early-onset amyloid deposition and cognitive deficits in transgenic mice expressing a double mutant form of amyloid precursor protein 695. J Biol Chem 276:21562–21570.

Choi SI, Vidal R, Frangione B, Levy E (2004) Axonal transport of British and Danish amyloid peptides via secretory vesicles. FASEB J 18:373–375.

Chyung JH, Raper DM, Selkoe DJ (2005) Gamma-secretase exists on the plasma membrane as an intact complex that accepts substrates and effects intramembrane cleavage. J Biol Chem 280:4383–4392.

De Strooper B (2003) Aph-1, Pen-2, and Nicastrin with Presenilin generate an active gamma-Secretase complex. Neuron 38:9–12.

De Strooper B (2005) Nicastrin: gatekeeper of the gamma-secretase complex. Cell 122:318–320.

Evin G, Sernee MF, Masters CL (2006) Inhibition of gamma-secretase as a therapeutic intervention for Alzheimer's disease: prospects, limitations and strategies. CNS Drugs 20:351–372.

Fotinopoulou A, Tsachaki M, Vlavaki M, Poulopoulos A, Rostagno A, Frangione B, Ghiso J, Efthimiopoulos S (2005) BRI2 interacts with amyloid precursor protein (APP) and regulates amyloid beta (Abeta) production. J Biol Chem 280:30768–30772.

Haass C, Selkoe DJ (2007) Soluble protein oligomers in neurodegeneration: lessons from the Alzheimer's amyloid beta-peptide. Nat Rev Mol Cell Biol 8:101–112.

Kim J, Miller VM, Levites Y, West KJ, Zwizinski CW, Moore BD, Troendle FJ, Bann M, Verbeeck C, Price RW, Smithson L, Sonoda L, Wagg K, Rangachari V, Zou F, Younkin SG, Graff-Radford N, Dickson D, Rosenberry T, Golde TE (2008) BRI2 (ITM2b) inhibits Aβ deposition *in vivo*. J Neurosci 28:6030–6036.

Kim SH, Wang R, Gordon DJ, Bass J, Steiner DF, Lynn DG, Thinakaran G, Meredith SC, Sisodia SS (1999) Furin mediates enhanced production of fibrillogenic ABri peptides in familial British dementia. Nat Neurosci 2:984–988.

Leissring MA, Murphy MP, Mead TR, Akbari Y, Sugarman MC, Jannatipour M, Anliker B, Müller U, Saftig P, De Strooper B, Wolfe MS, Golde TE, LaFerla FM (2002) A physiologic signaling role for the gamma-secretase-derived intracellular fragment of APP. Proc Natl Acad Sci U S A 99:4697–4702.

Li Q, Südhof TC (2004) Cleavage of amyloid-beta precursor protein and amyloid-beta precursor-like protein by BACE 1. J Biol Chem 279:10542–10550.

Matsuda S, Giliberto L, Matsuda Y, Davies P, McGowan E, Pickford F, Ghiso J, Frangione B, D'Adamio L (2005) The familial dementia BRI2 gene binds the Alzheimer gene amyloid-beta precursor protein and inhibits amyloid-beta production. J Biol Chem 280:28912–28916.

Mayford M, Bach ME, Kandel E (1996) CaMKII function in the nervous system explored from a genetic perspective. Cold Spring Harb Symp Quant Biol 61:219–224.

Minopoli G, Zambrano N, Russo T (2006) The cytosolic domain of APP and its possible role in the pathogenesis of Alzheimer's disease. Ital J Biochem 55:205–211.

Passer B, Pellegrini L, Russo C, Siegel RM, Lenardo MJ, Schettini G, Bachmann M, Tabaton M, D'Adamio L (2000) Generation of an apoptotic intracellular peptide by gamma-secretase cleavage of Alzheimer's amyloid beta protein precursor. J Alzheimers Dis 2:289–301.

Pickford F, Coomaraswamy J, Jucker M, McGowan E (2006) Modeling familial British dementia in transgenic mice. Brain Pathol 16:80–85.

Revesz T, Holton JL, Lashley T, Plant G, Rostagno A, Ghiso J, Frangione B (2002) Sporadic and familial cerebral amyloid angiopathies. Brain Pathol 12:343–357.

Roncarati R, Sestan N, Scheinfeld MH, Berechid BE, Lopez PA, Meucci O, McGlade JC, Rakic P, D'Adamio L (2002) The gamma-secretase-generated intracellular domain of beta-amyloid precursor protein binds

Numb and inhibits Notch signaling. Proc Natl Acad Sci U S A 99:7102–7107.

Saura CA, Choi SY, Beglopoulos V, Malkani S, Zhang D, Shankaranarayana Rao BS, Chattarji S, Kelleher RJ 3rd, Kandel ER, Duff K, Kirkwood A, Shen J (2004) Loss of presenilin function causes impairments of memory and synaptic plasticity followed by age-dependent neurodegeneration. Neuron 42:23–36.

Savonenko AV, Xu GM, Price DL, Borchelt DR, Markowska AL (2003) Normal cognitive behavior in two distinct congenic lines of transgenic mice hyperexpressing mutant APP SWE. Neurobiol Dis 12:194–211.

Scheinfeld MH, Ghersi E, Laky K, Fowlkes BJ, D'Adamio L (2002) Processing of beta-amyloid precursor-like protein-1 and -2 by gamma-secretase regulates transcription. J Biol Chem 277:44195–44201.

Selkoe D, Kopan R (2003) Notch and Presenilin: regulated intramembrane proteolysis links development and degeneration. Annu Rev Neurosci 26:565–597.

Selkoe DJ, Podlisny MB (2002) Deciphering the genetic basis of Alzheimer's disease. Annu Rev Genomics Hum Genet 3:67–99.

Sestan N, Artavanis-Tsakonas S, Rakic P (1999) Contact-dependent inhibition of cortical neurite growth mediated by notch signaling. Science 286:741–746.

Shah S, Lee SF, Tabuchi K, Hao YH, Yu C, LaPlant Q, Ball H, Dann CE 3rd, Südhof T, Yu G (2005) Nicastrin functions as a gamma-secretase-substrate receptor. Cell 122:435–447.

Shen J, Kelleher RJ 3rd (2007) The presenilin hypothesis of Alzheimer's disease: evidence for a loss-of-function pathogenic mechanism. Proc Natl Acad Sci U S A 104:403–409.

Sisodia SS, St. George-Hyslop PH (2002) gamma-Secretase, Notch, Abeta and Alzheimer's disease: where do the presenilins fit in? Nat Rev Neurosci 3:281–290.

Vidal R, Frangione B, Rostagno A, Mead S, Révész T, Plant G, Ghiso J (1999) A stop-codon mutation in the BRI gene associated with familial British dementia. Nature 399:776–781.

Vidal R, Revesz T, Rostagno A, Kim E, Holton JL, Bek T, Bojsen-Møller M, Braendgaard H, Plant G, Ghiso J, Frangione B (2000) A decamer duplication in the 3′ region of the BRI gene originates an amyloid peptide that is associated with dementia in a Danish kindred. Proc Natl Acad Sci U S A 97:4920–4925.

Yu G, Nishimura M, Arawaka S, Levitan D, Zhang L, Tandon A, Song YQ, Rogaeva E, Chen F, Kawarai T, Supala A, Levesque L, Yu H, Yang DS, Holmes E, Milman P, Liang Y, Zhang DM, Xu DH, Sato C, et al. (2000) Nicastrin modulates presenilin-mediated notch/glp-1 signal transduction and betaAPP processing. Nature 407:48–54.

Zazzeroni F, Papa S, Algeciras-Schimnich A, Alvarez K, Melis T, Bubici C, Majewski N, Hay N, De Smaele E, Peter ME, Franzoso G (2003) Gadd45 beta mediates the protective effects of CD40 costimulation against Fas-induced apoptosis. Blood 102:3270–3279.